

Development of Highly Efficient Bimetallic Metal Organic Frameworks for the Extraction of Pd(II) from Aqueous Solutions

Somnath Sengupta,¹ S.B. Shrikala,² Nitin Gumber,³ A. Suneesh,¹ B. Sreenivasulu,^{1,4} C. V. S. Brahmananda Rao,^{1,4}*

¹ Material Chemistry and Metal Fuel Cycle Group, Indira Gandhi Centre for Atomic Research, Kalpakkam– 603 102, Tamil Nadu, India.

² Amrita Vishwa Vidyapeetham, Coimbatore, Tamil Nadu, India.

³ Fuel Chemistry Division, Bhabha Atomic Research Centre, Mumbai-400085, India

⁴ Homi Bhabha National Institute, Indira Gandhi Centre for Atomic Research, Kalpakkam – 603 102, Tamil Nadu, India.

Corresponding author:

Dr. B. Sreenivasulu,
Fuel Chemistry Division,
Materials Chemistry and Metal Fuel Cycle Group,
Indira Gandhi Centre for Atomic Research,
Kalpakkam – 603102,
Tamil Nadu, India.
Tel. +91 44 27480055 – 24287
Email: bsrinu@igcar.gov.in

Determination of Pd(II) concentration using UV-vis spectroscopy

The colorimetric determination of Pd(II) was done using Thorin indicator as chromogenic agent, which tends to form 1:1 violet complex with divalent palladium which shows λ_{max} around 540 nm. 1 mL of 0.05 % (w/V) thorin indicator was used for the studies. pH of the solution to be analyzed was maintained at 3.7 using sodium acetate-acetic acid buffer. A series of solutions ranging from 1 ppm to 10 ppm was prepared from a standard Pd(II) stock solution of concentration 1 g/L. The calibration was done with these standard solutions which yielded a linear calibration plot. The value of molar extinction coefficient, obtained from the slope of calibration plot was found to be $6598.04 \text{ L mol}^{-1} \text{ cm}^{-1}$. Similar procedure for palladium(II) determination was reported in literature.¹

PXRD

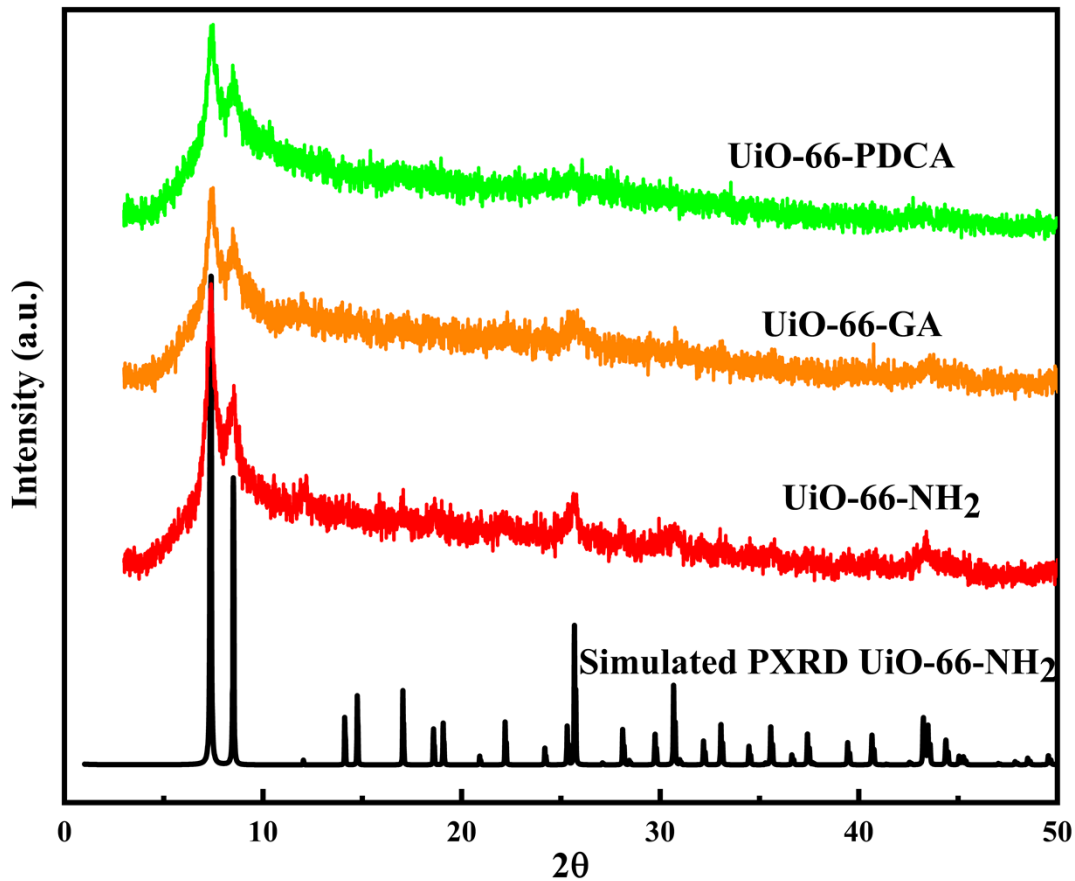


Fig. S1 PXRD of UiO-66-NH_2 , UiO-66-GA and UiO-66-PDCA

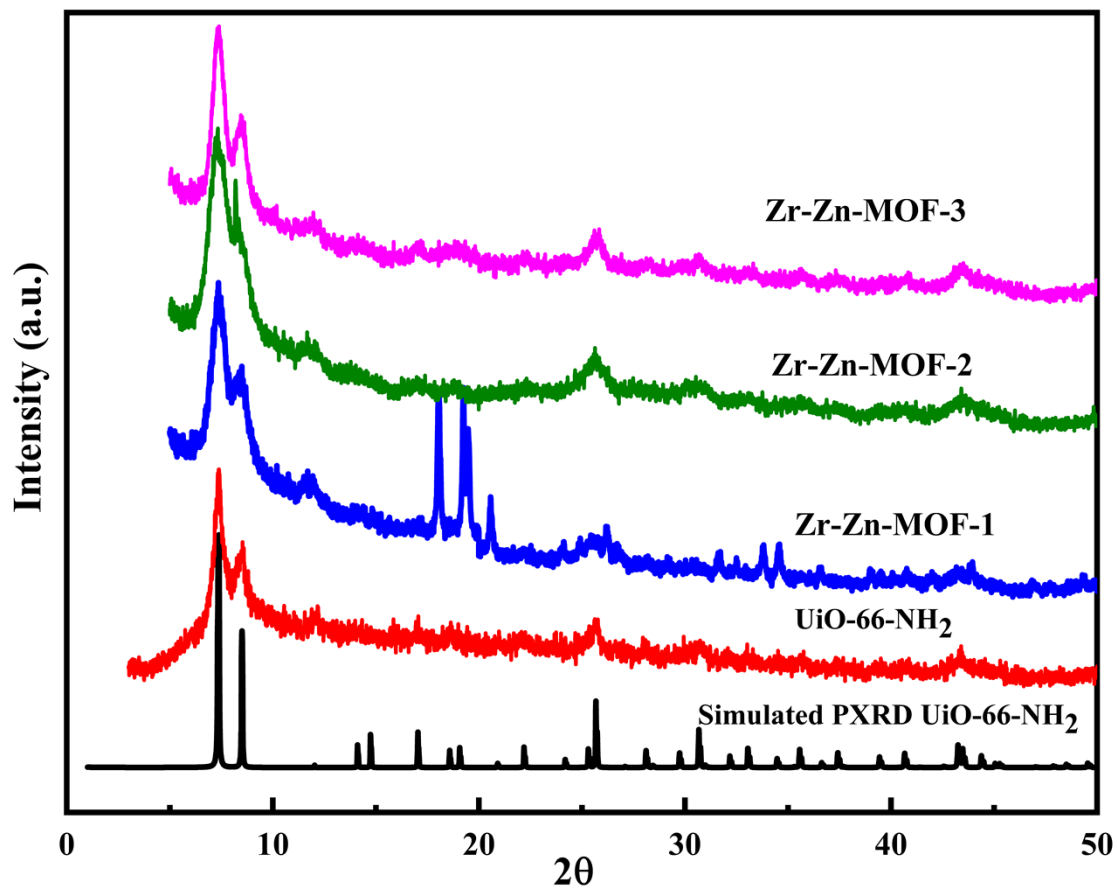


Fig. S2 PXRD of UiO-66-NH₂ and bimetallic MOFs

BET Surface Area Analysis

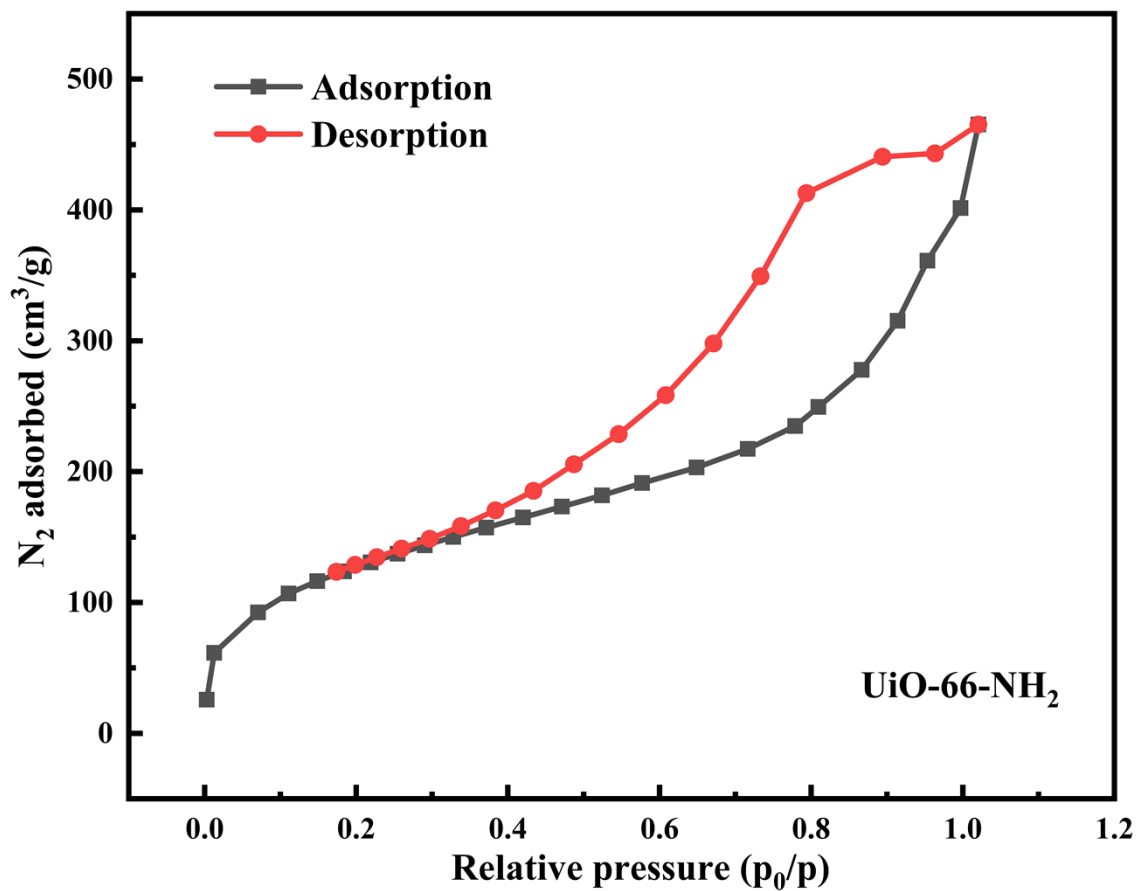


Fig. S3 N₂ adsorption-desorption isotherm at 77 K for UiO-66-NH₂

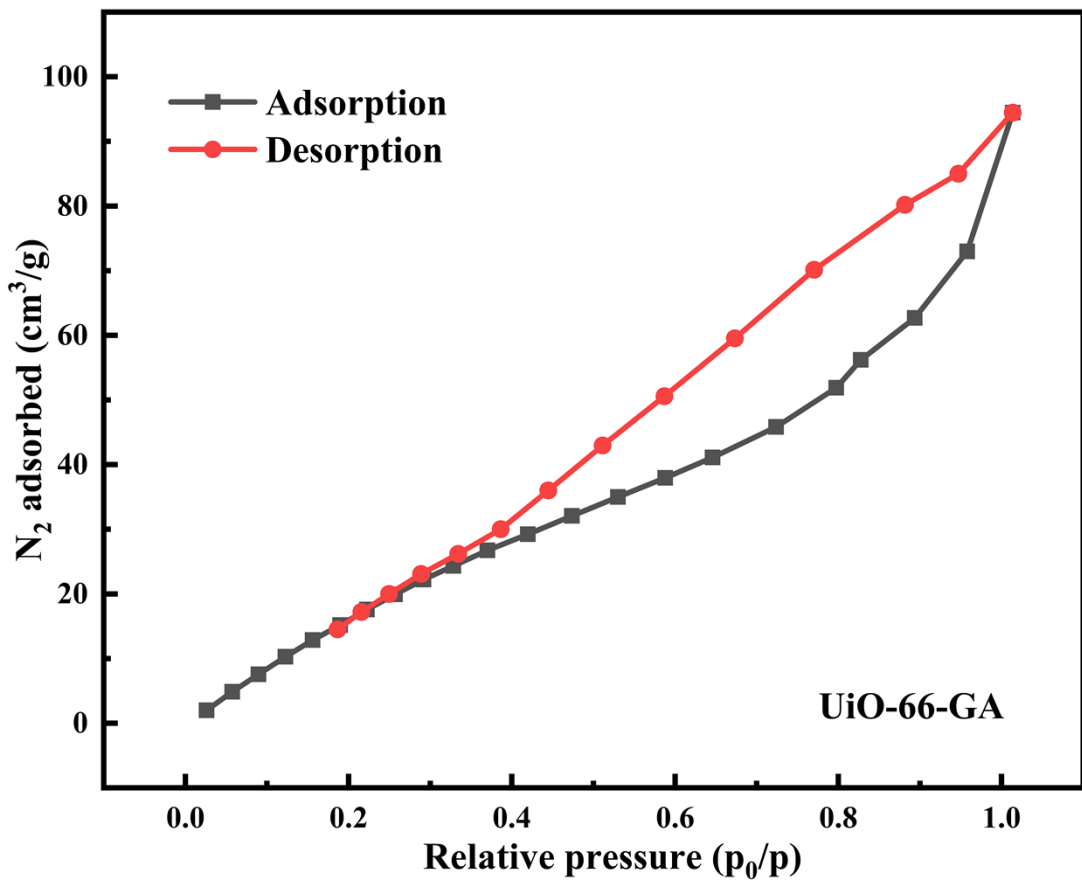


Fig. S4 N₂ adsorption-desorption isotherm at 77 K for UiO-66-GA

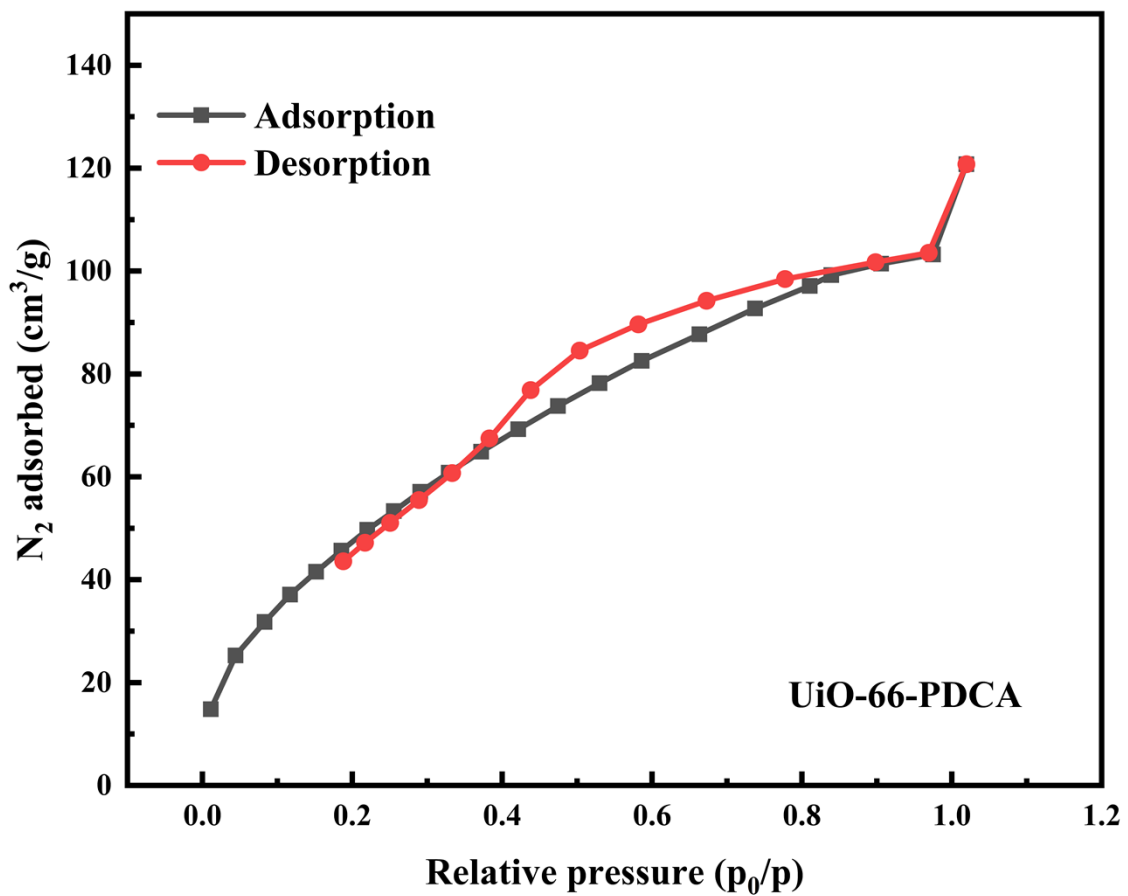


Fig. S5 N₂ adsorption-desorption isotherm at 77 K for UiO-66-PDCA

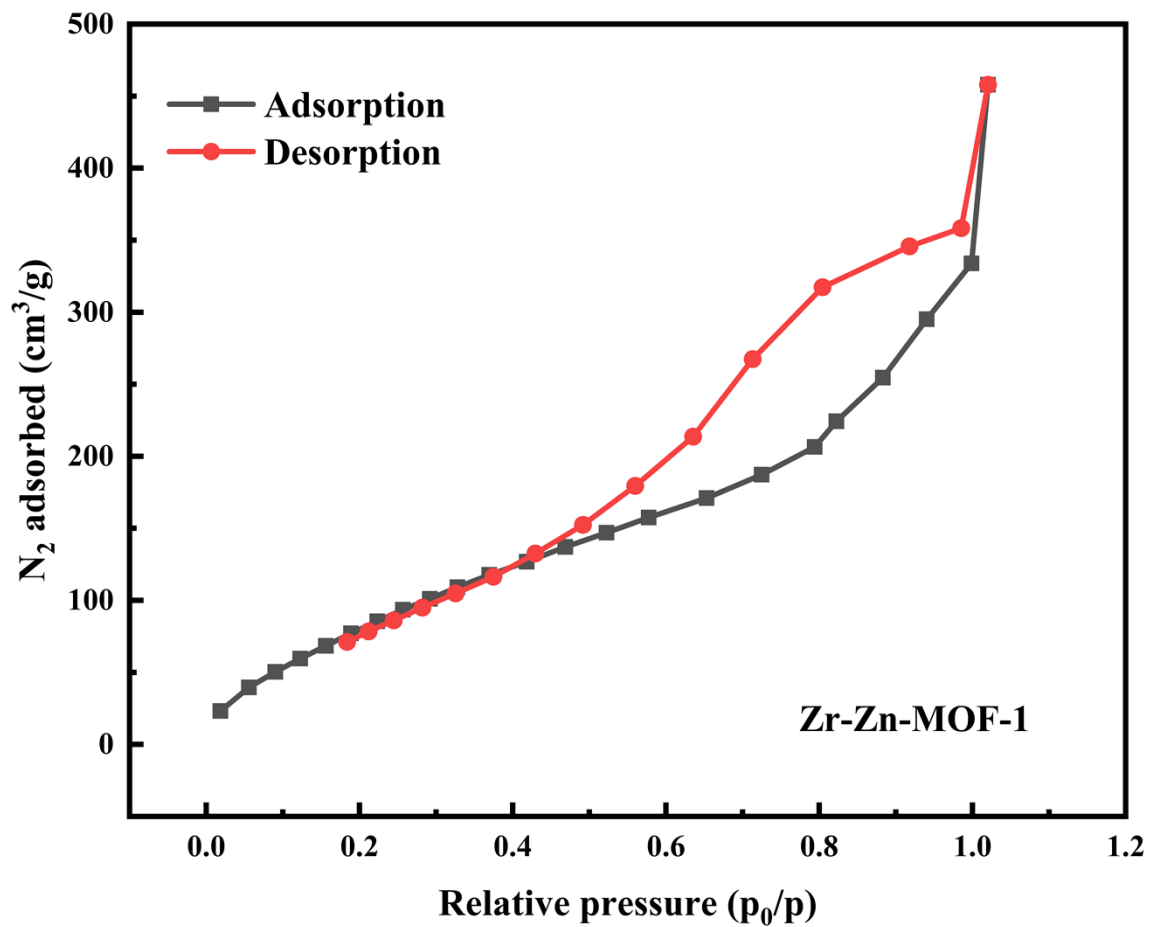


Fig. S6 N₂ adsorption-desorption isotherm at 77 K for Zr-Zn-MOF-1

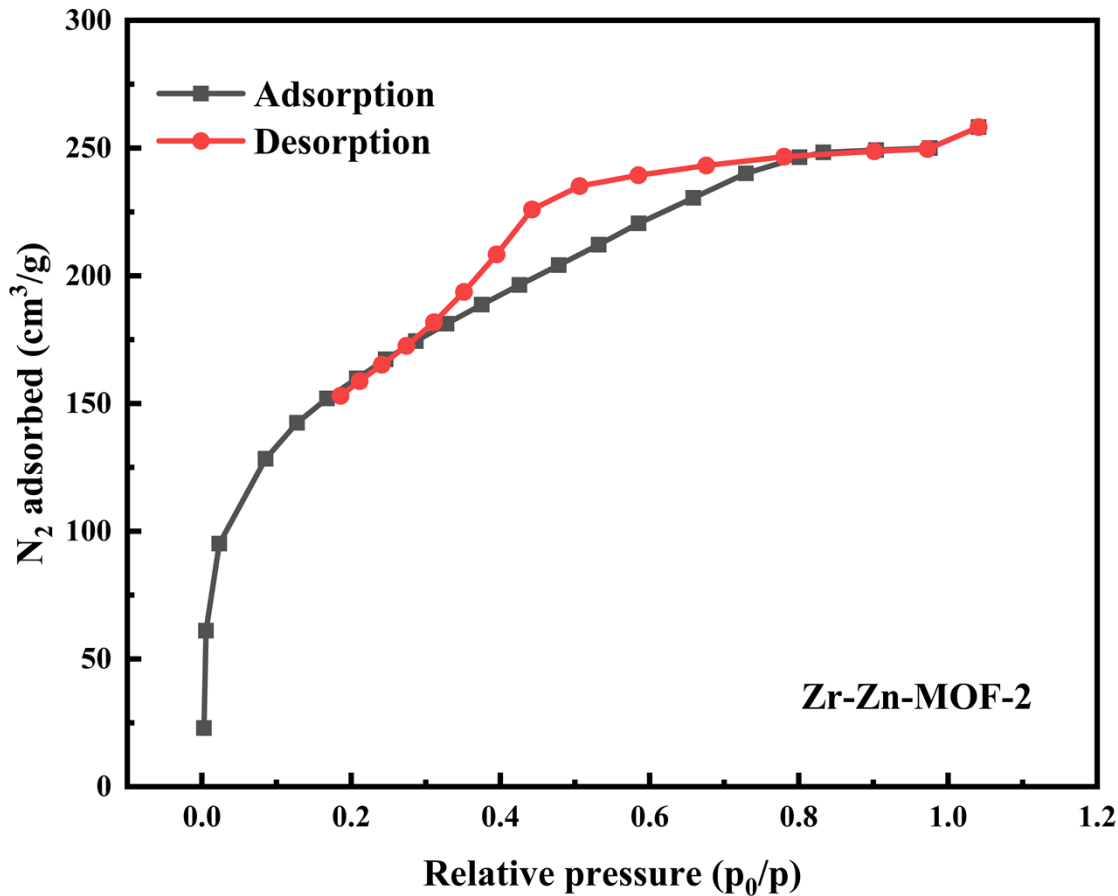


Fig. S7 N₂ adsorption-desorption isotherm at 77 K for Zr-Zn-MOF-2

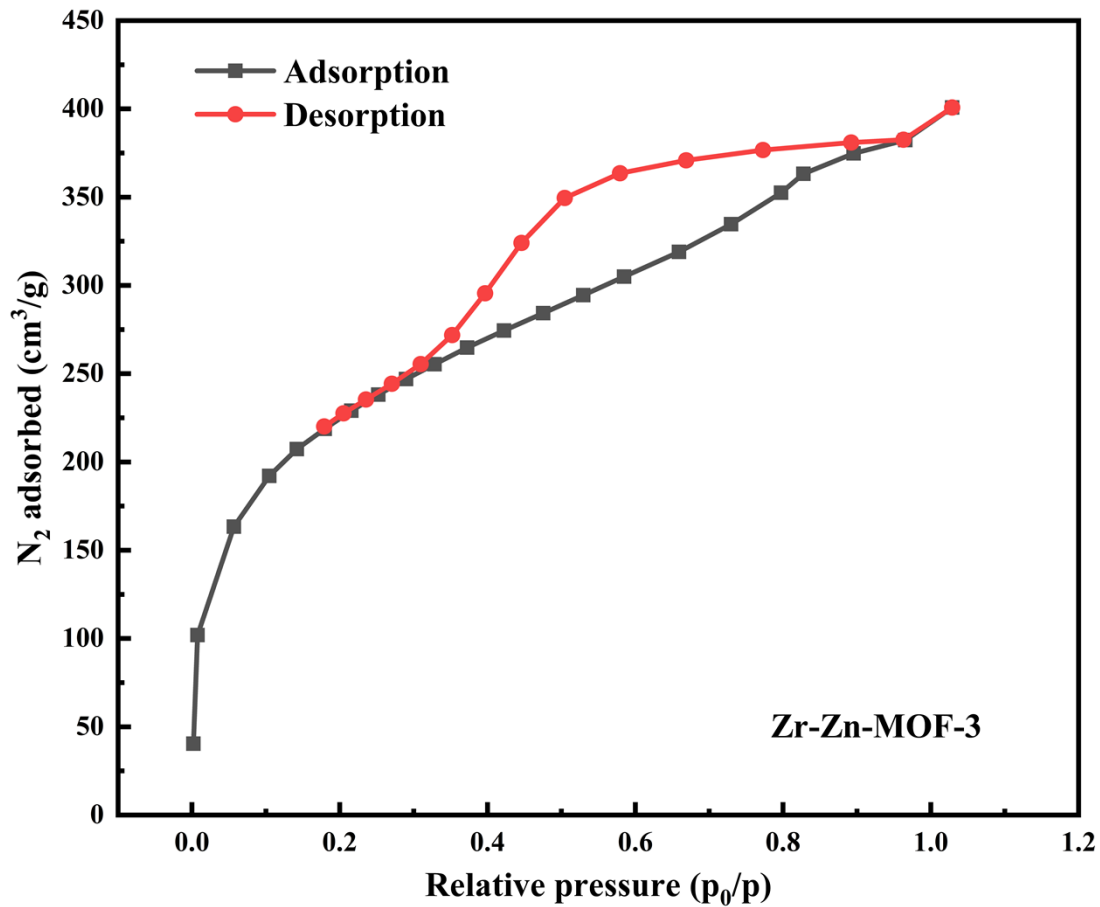
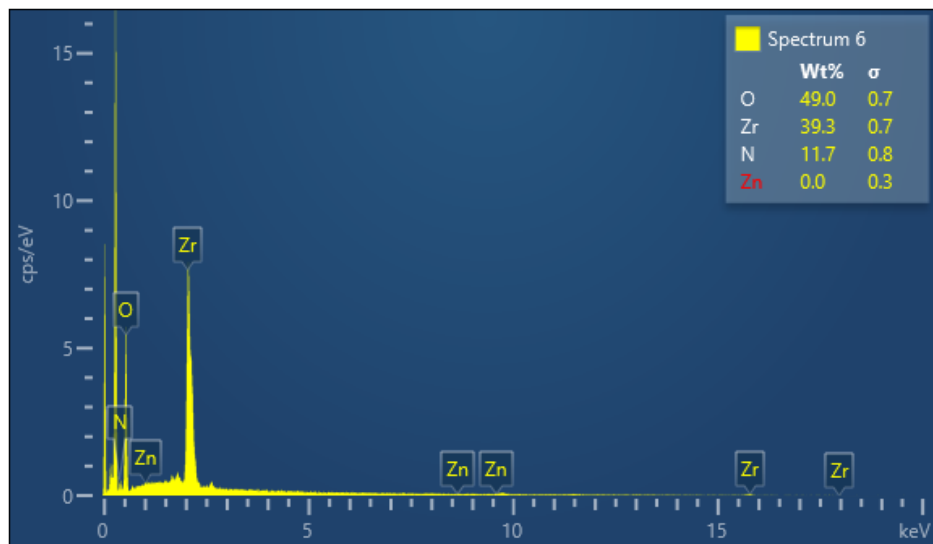
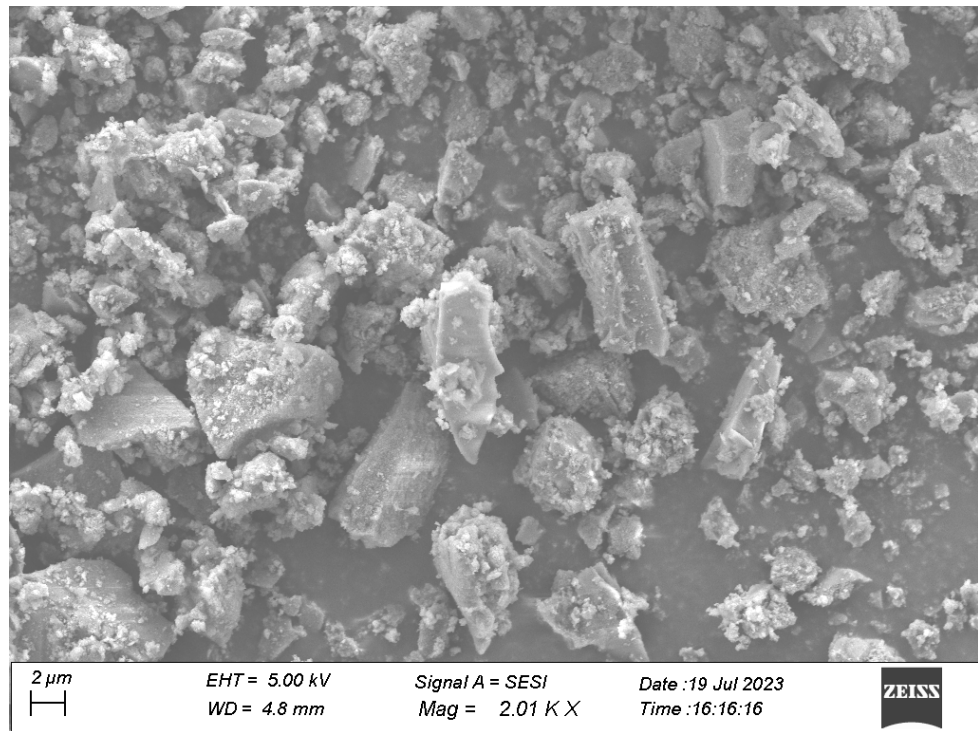


Fig. S8 N₂ adsorption-desorption isotherm at 77 K for Zr-Zn-MOF-3

SEM-EDX Analysis

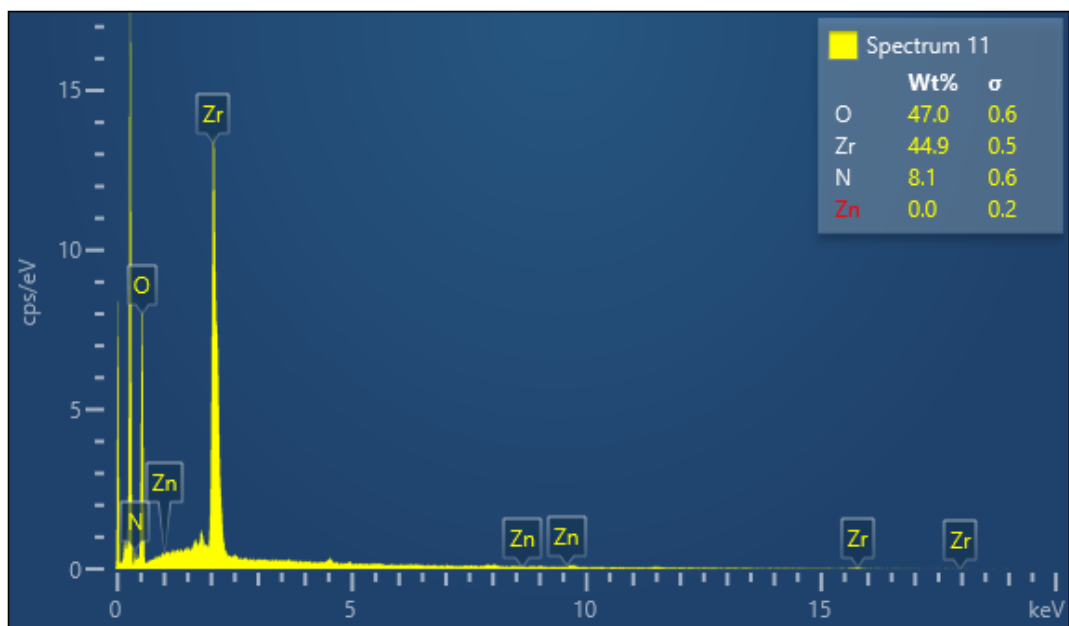


(a)

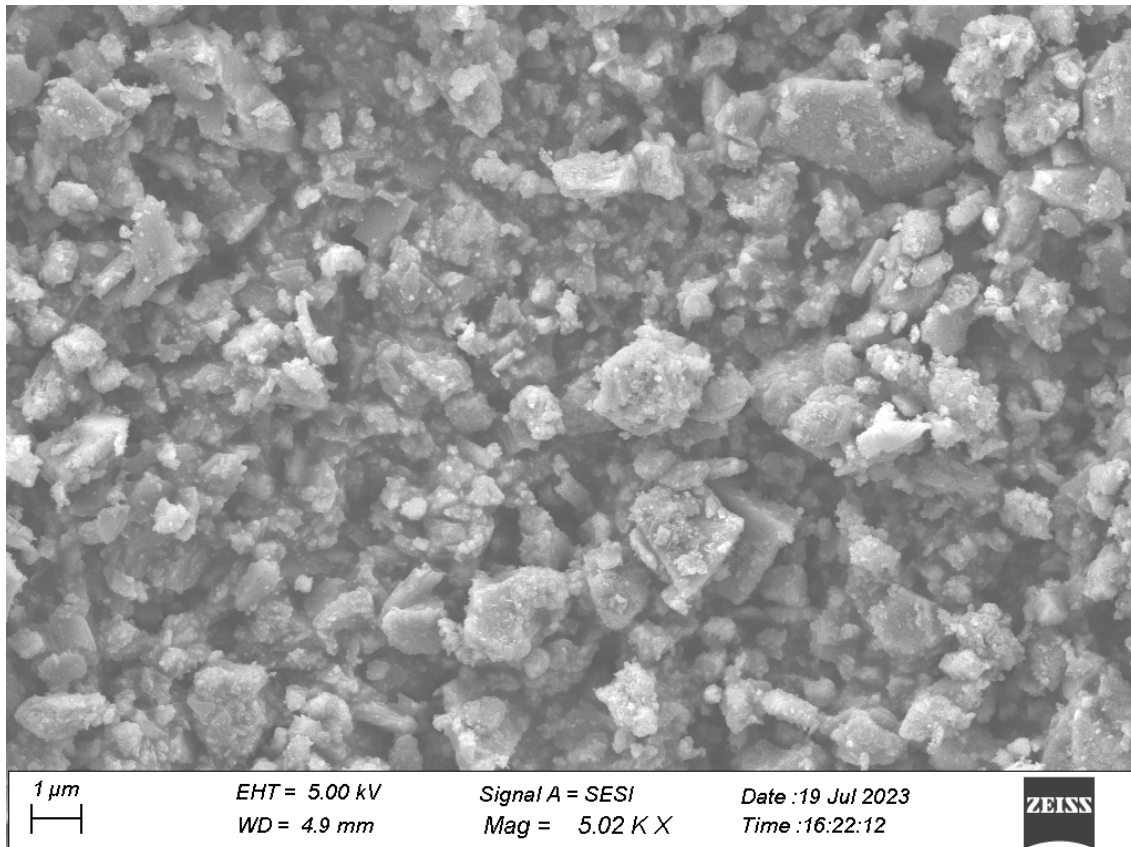


(b)

Fig. S9(a) EDX spectra and (b) SEM image of UiO-66-NH₂.

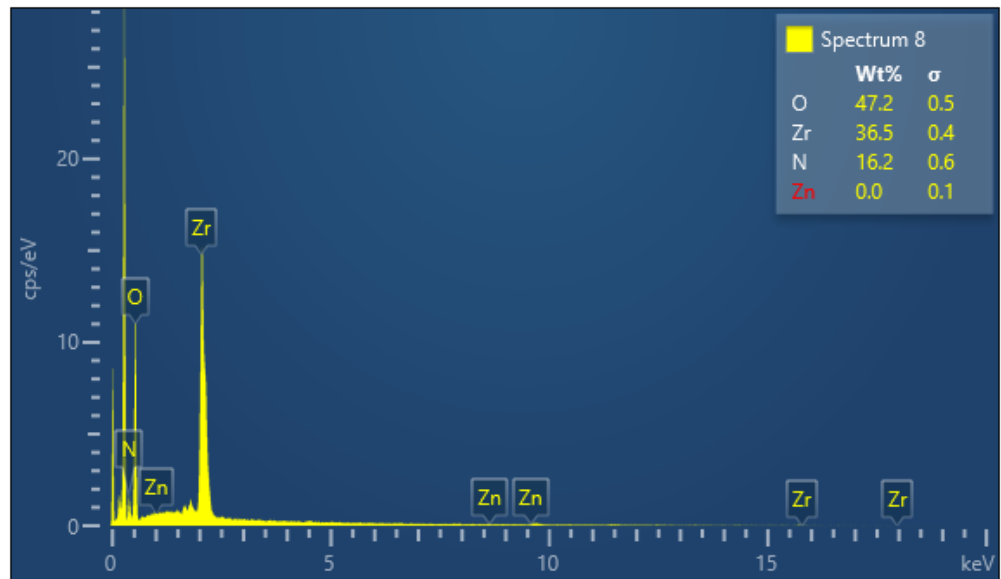


(a)

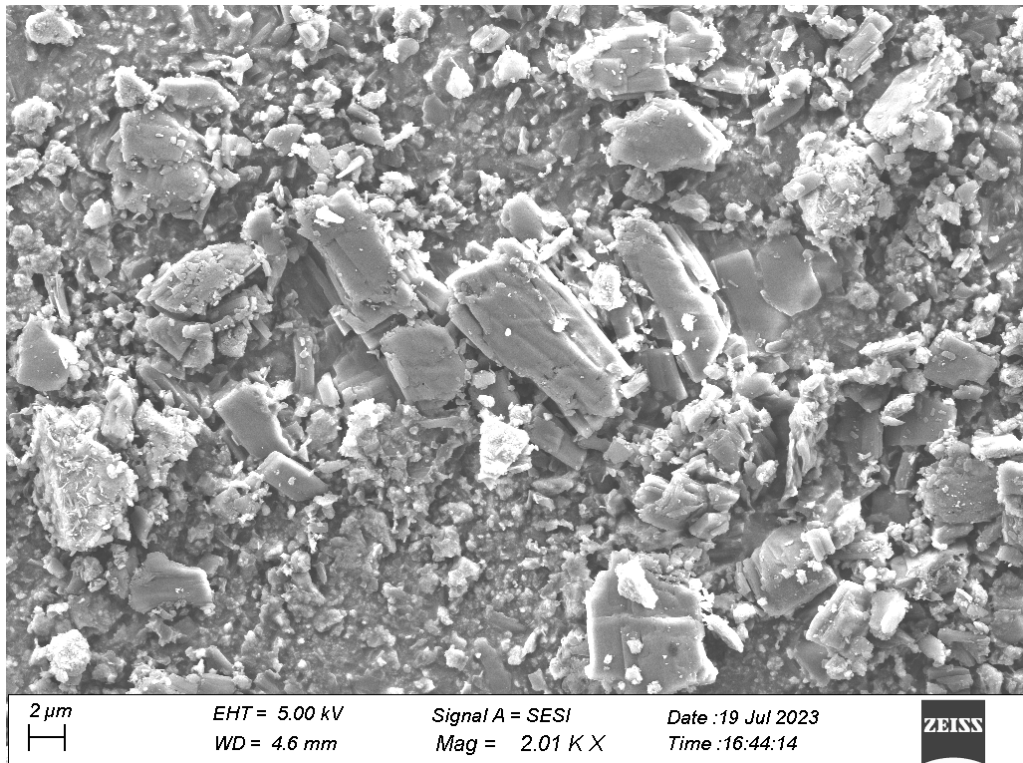


(b)

Fig. S10(a) EDX spectra and (b) SEM image of UiO-66-GA.

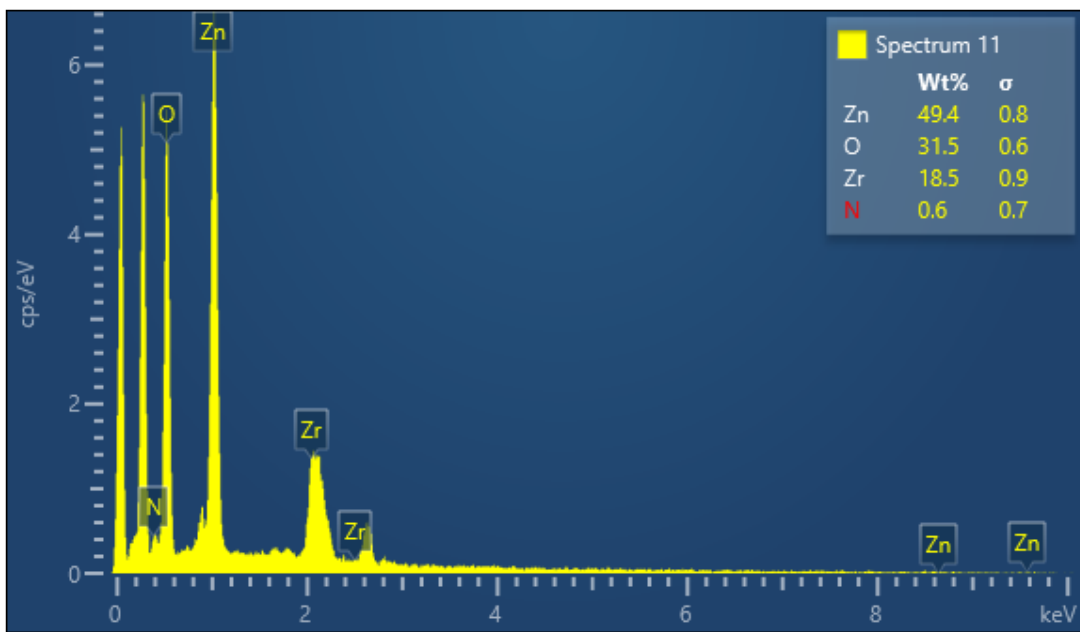


(a)

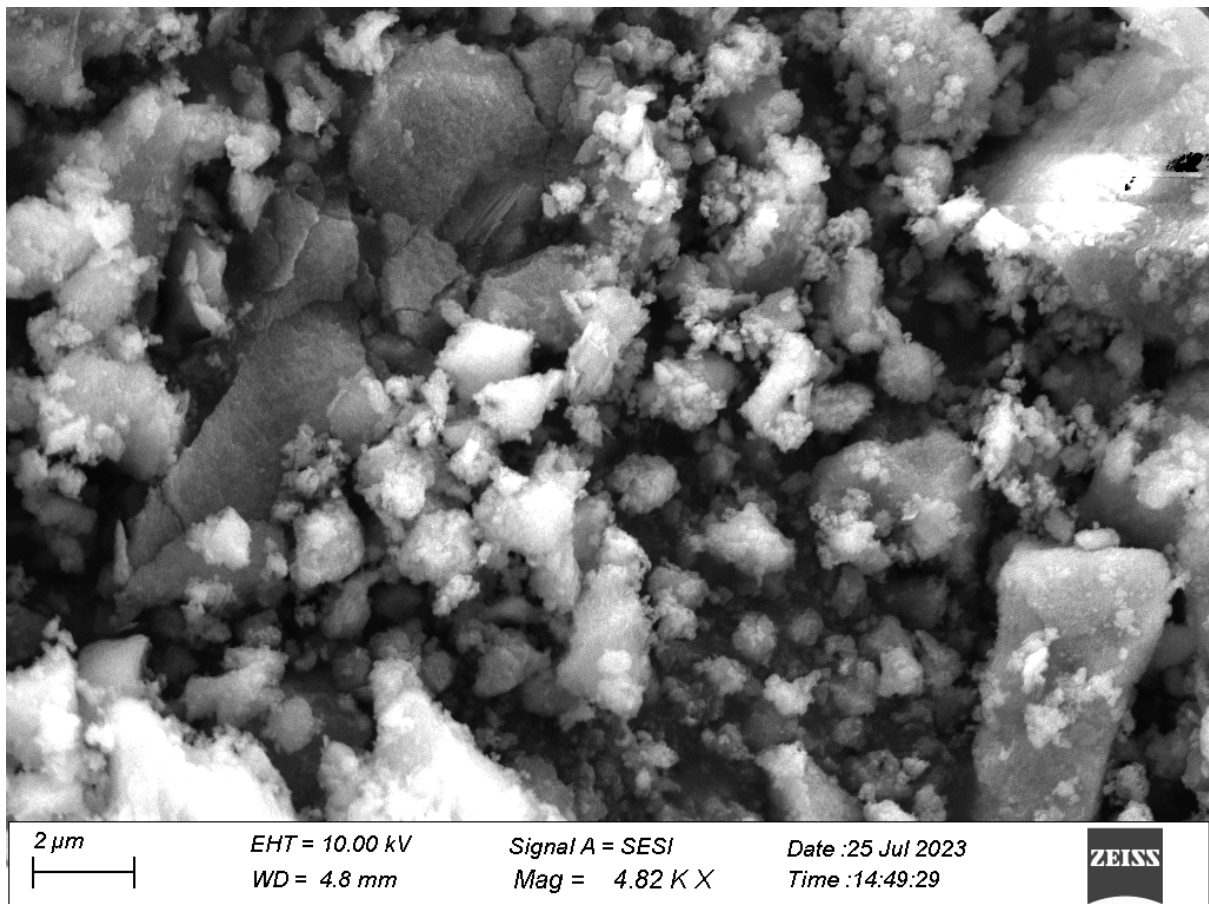


(b)

Fig. S11(a) EDX spectra and (b) SEM image of UiO-66-PDCA.

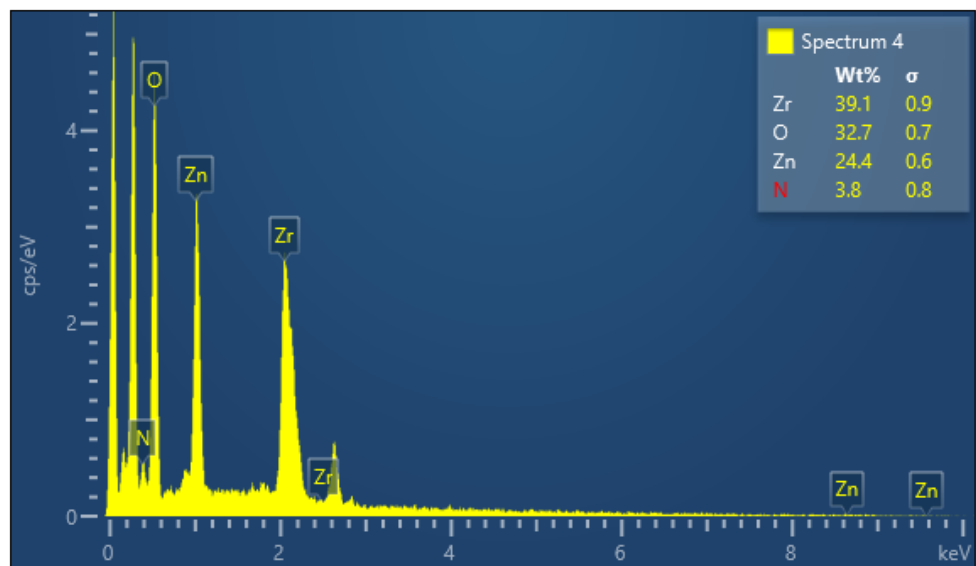


(a)

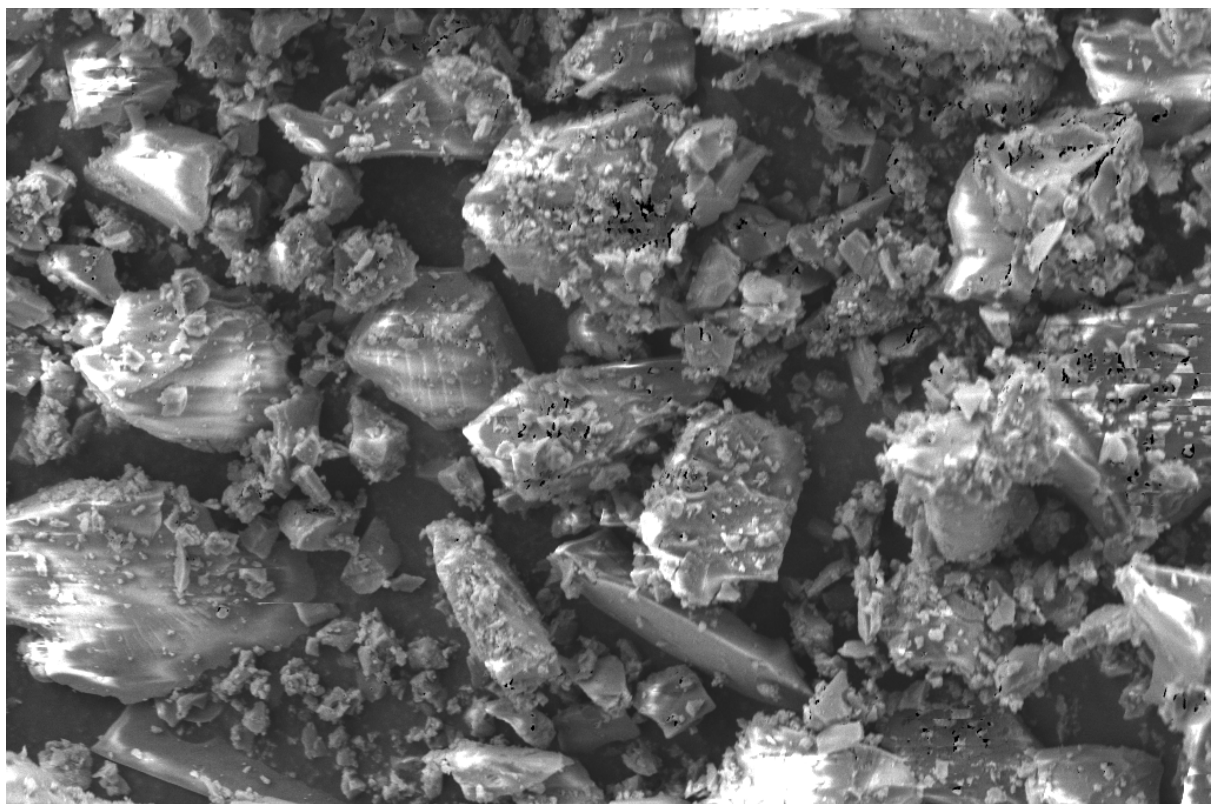


(b)

Fig. S12(a) EDX spectra and (b) SEM image of Zr-Zn-MOF-1.



(a)

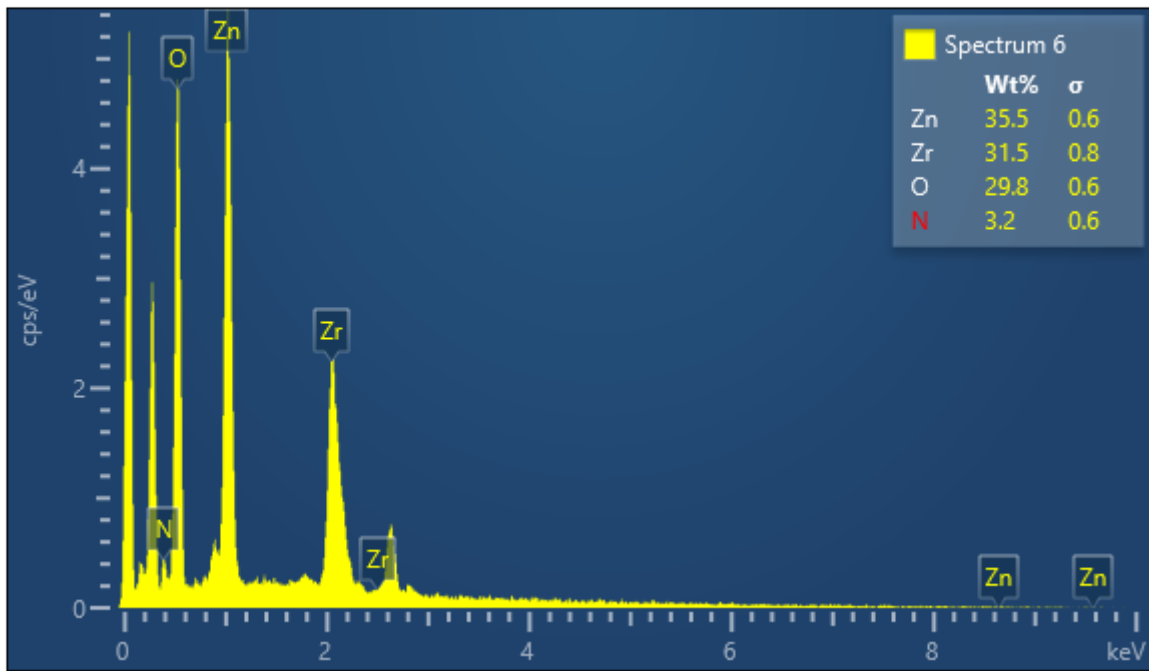


10 μ m	EHT = 5.00 kV	Signal A = SESI	Date :25 Jul 2023
	WD = 5.1 mm	Mag = 1.43 K X	Time :15:36:14

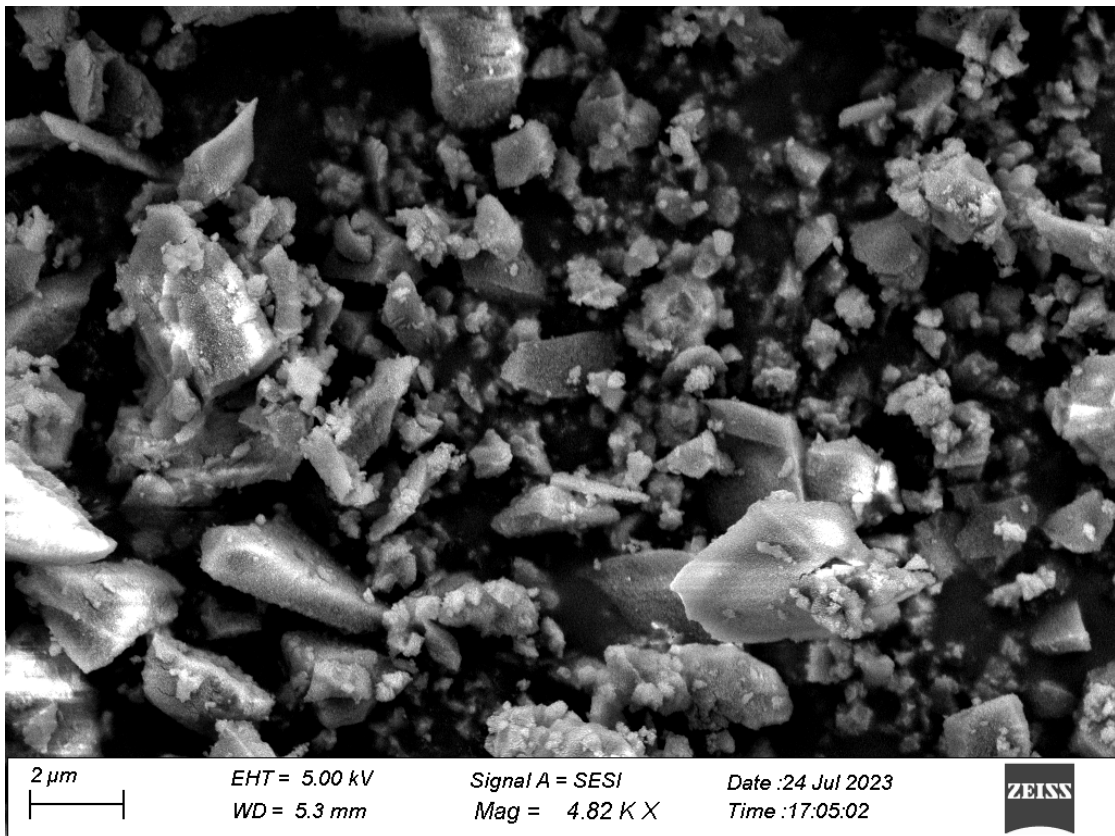


(b)

Fig. S13(a) EDX spectra and (b) SEM image of Zr-Zn-MOF-2.



(a)



(b)

Fig. S14(a) EDX spectra and (b) SEM image of Zr-Zn-MOF-3.

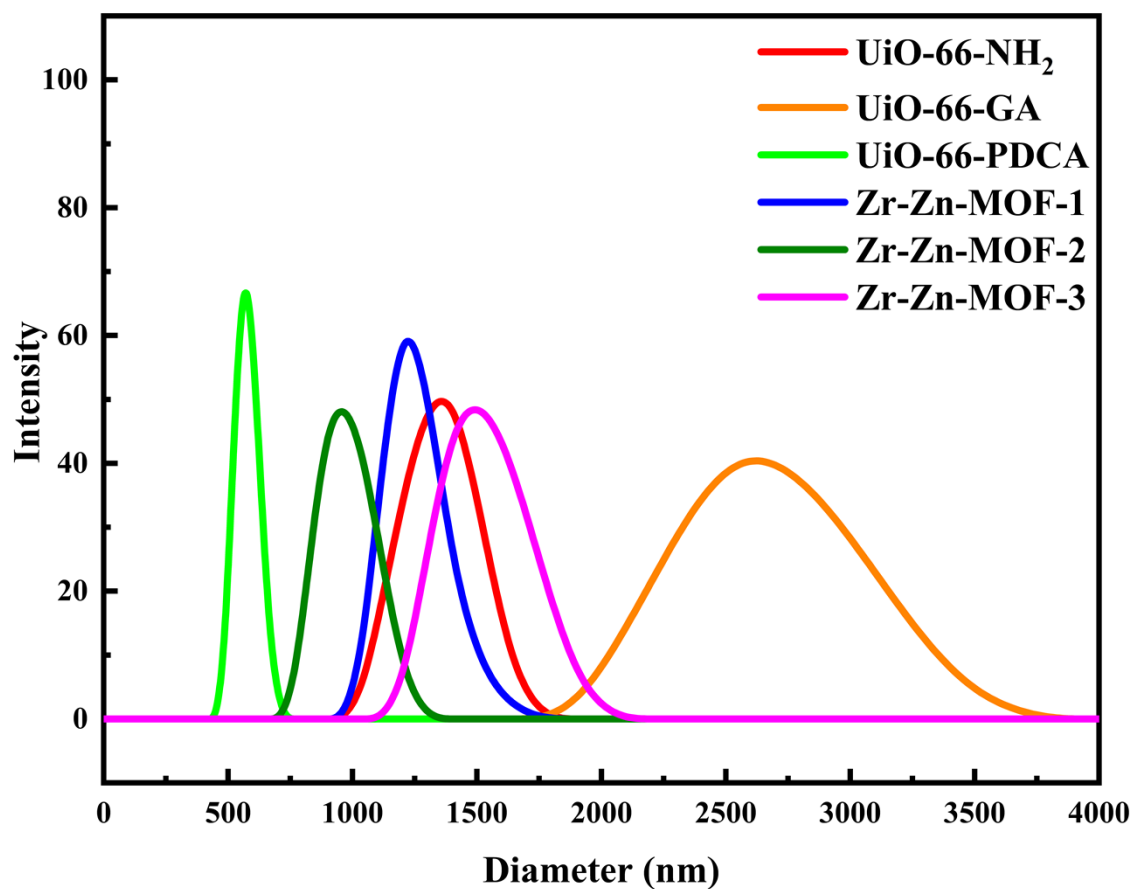
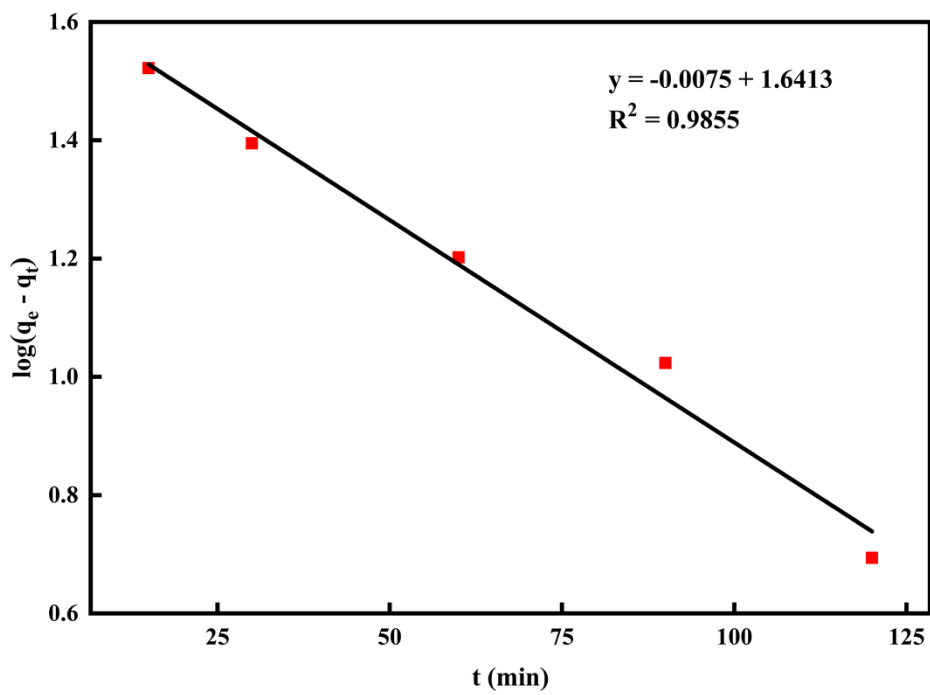
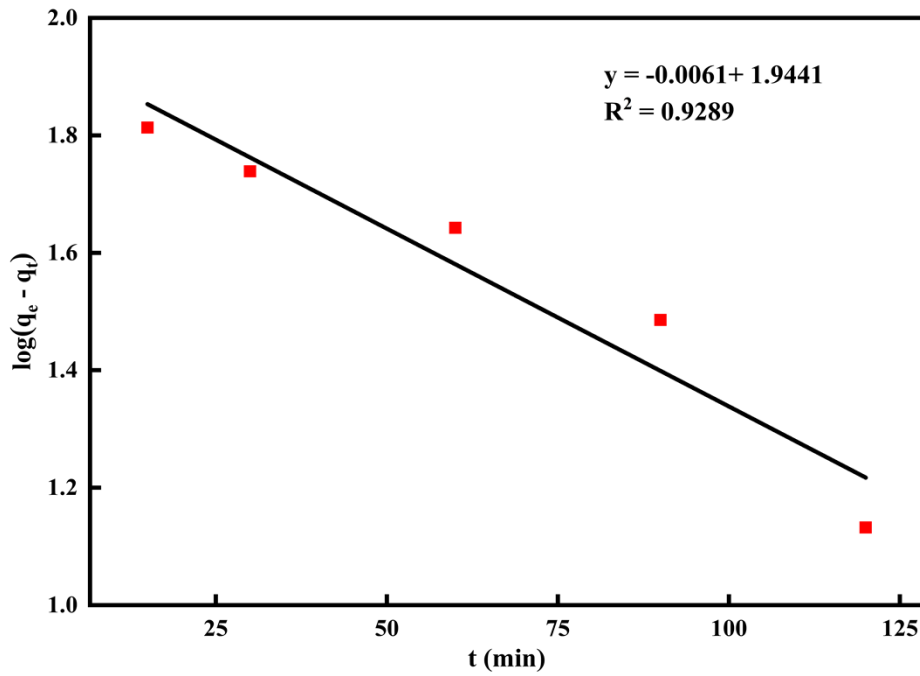


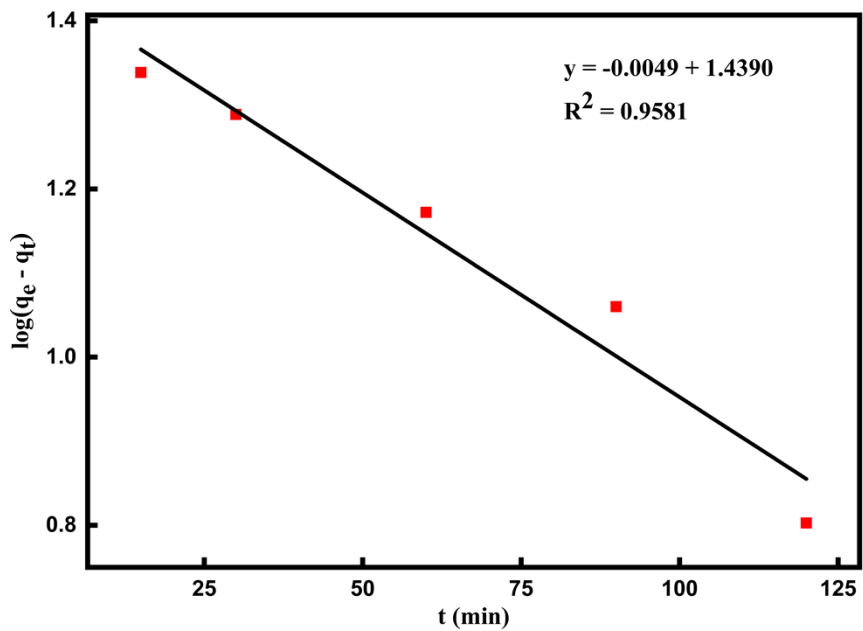
Fig. S15 Dynamic light scattering (DLS) particle size distributions for the MOF samples dispersed in aqueous solution.



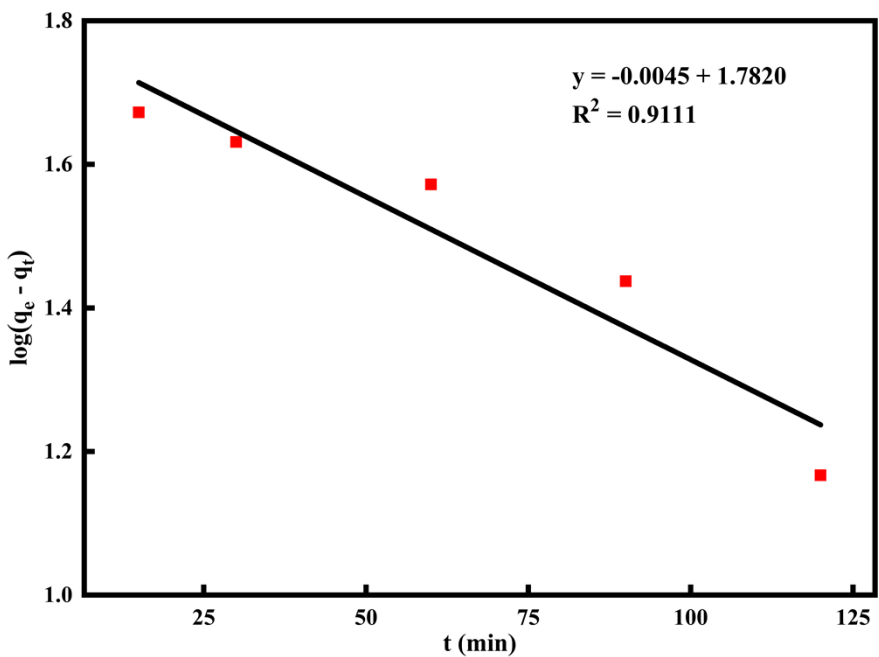
(a)



(b)

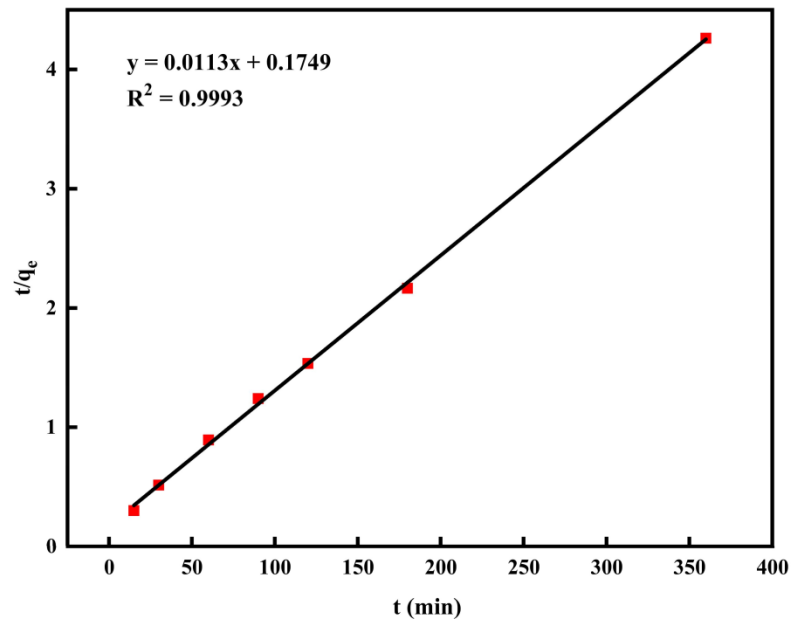


(c)

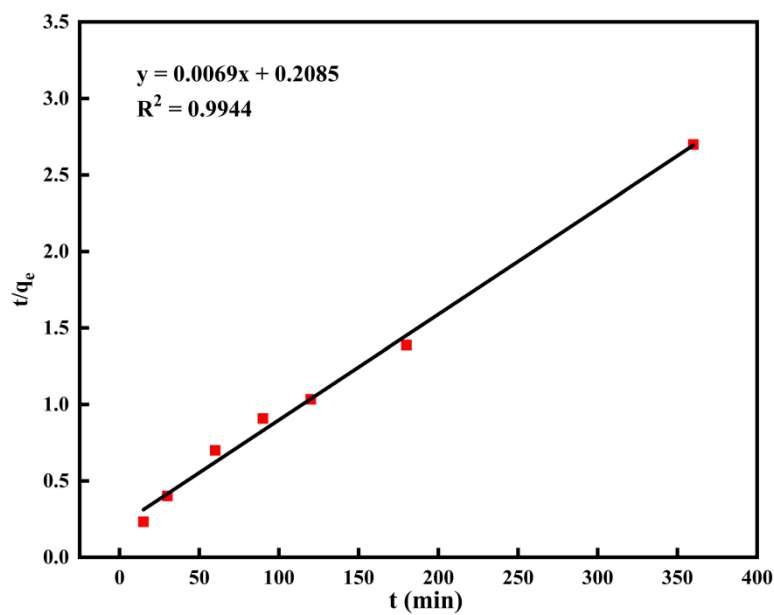


(d)

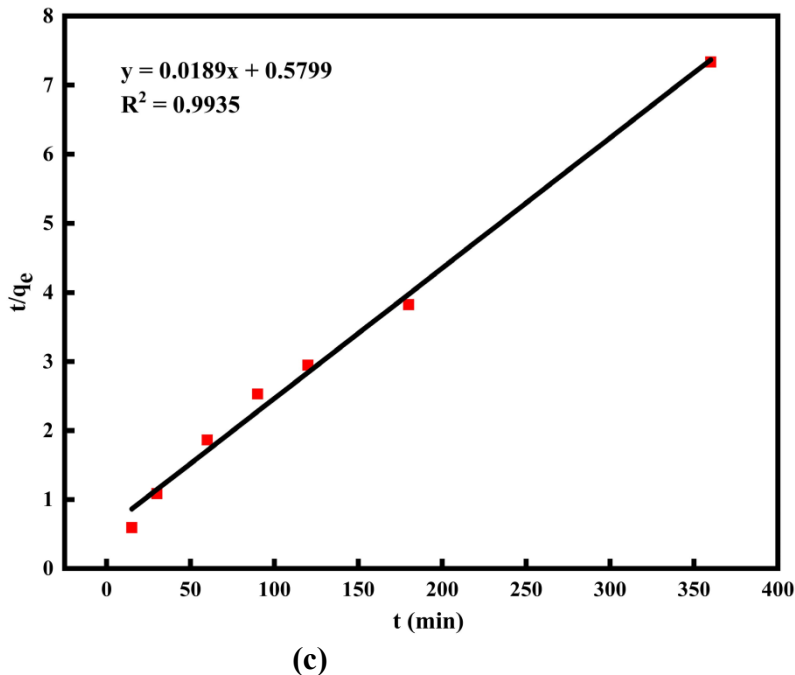
Fig. S16 Linear plots for pseudo-first order kinetics for the adsorption of palladium(II) on different MOFs (a) UiO-66-NH₂ (b) Zr-Zn-MOF-1 (c) Zr-Zn-MOF-2 (d) Zr-Zn-MOF-3



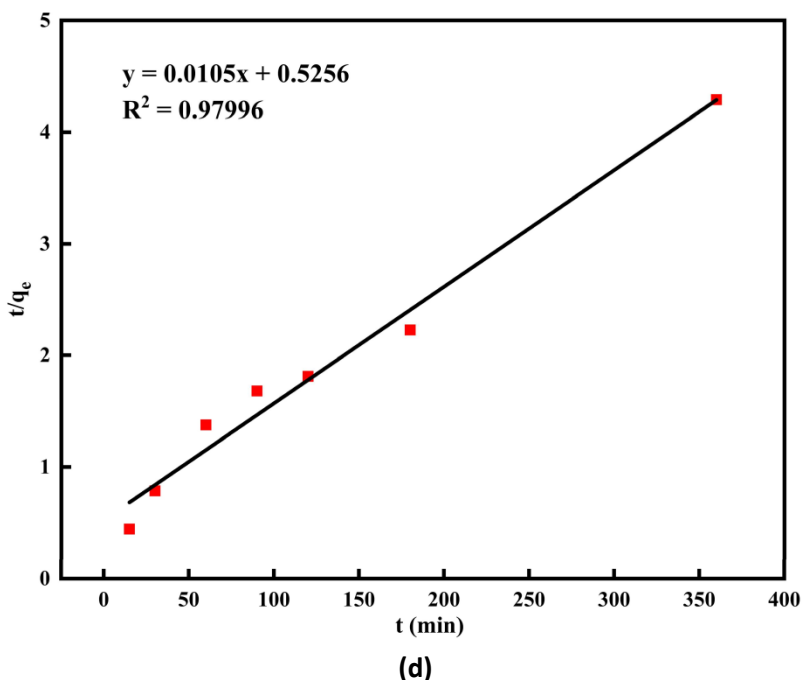
(a)



(b)

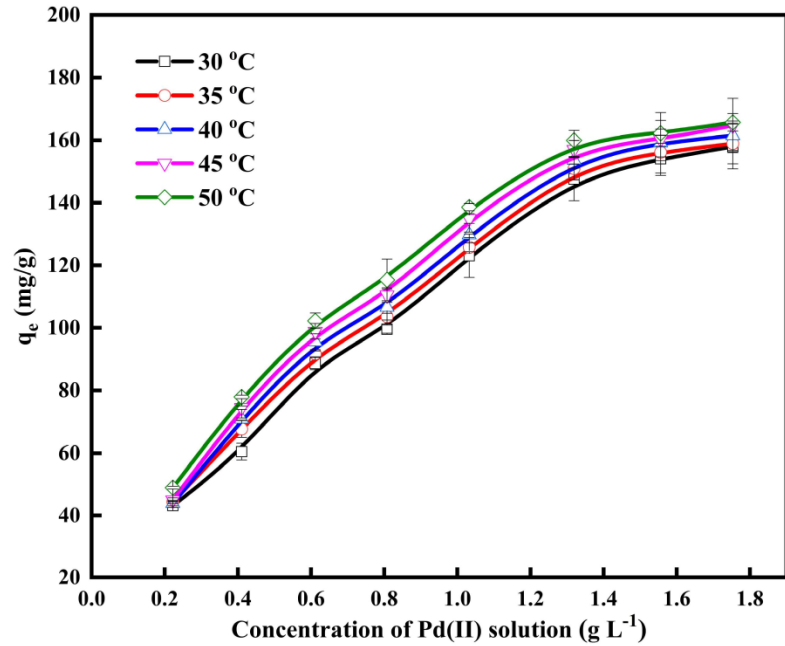


(c)

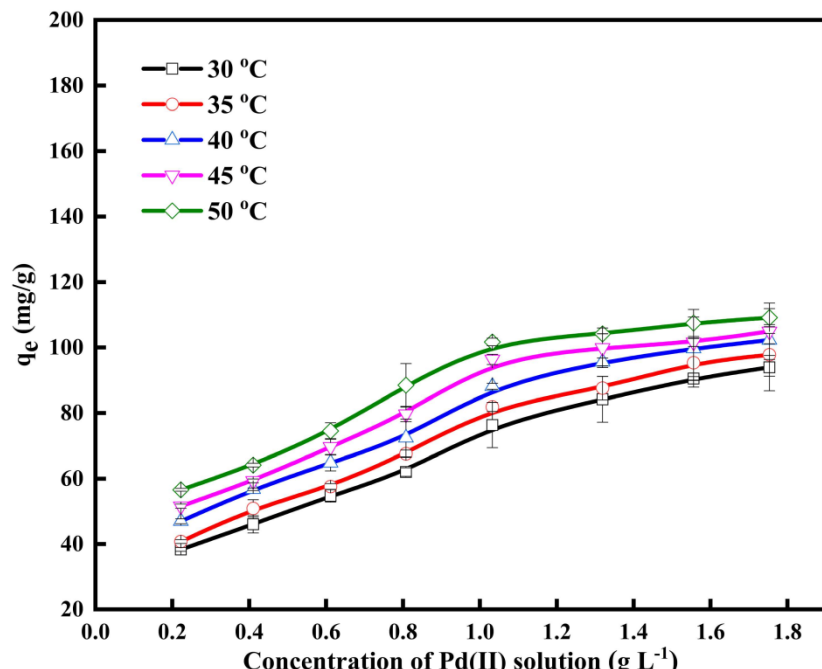


(d)

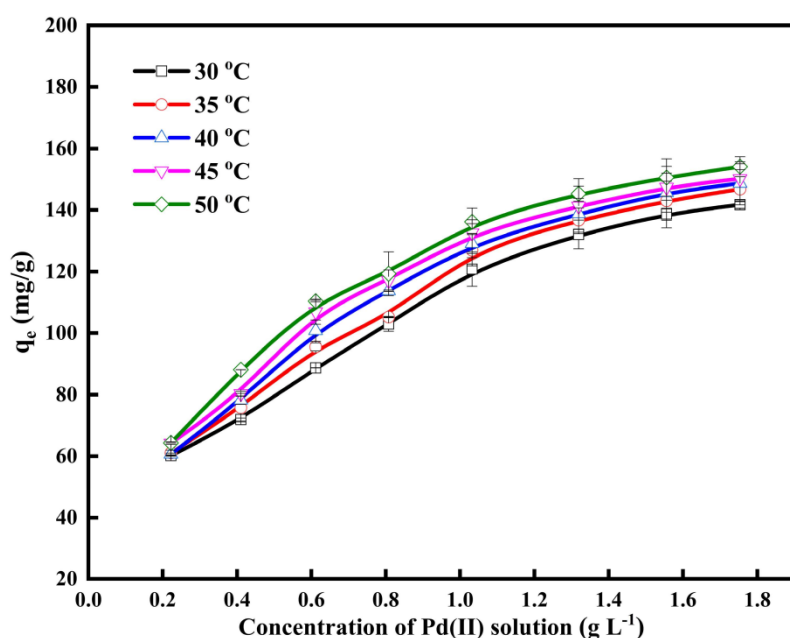
Fig. S17 Linear plots for pseudo-second order kinetics for the adsorption of palladium (II) on different MOFs (a) UiO-66-NH₂ (b) Zr-Zn-MOF-1 (c) Zr-Zn-MOF-2 (d) Zr-Zn-MOF-3



(a)

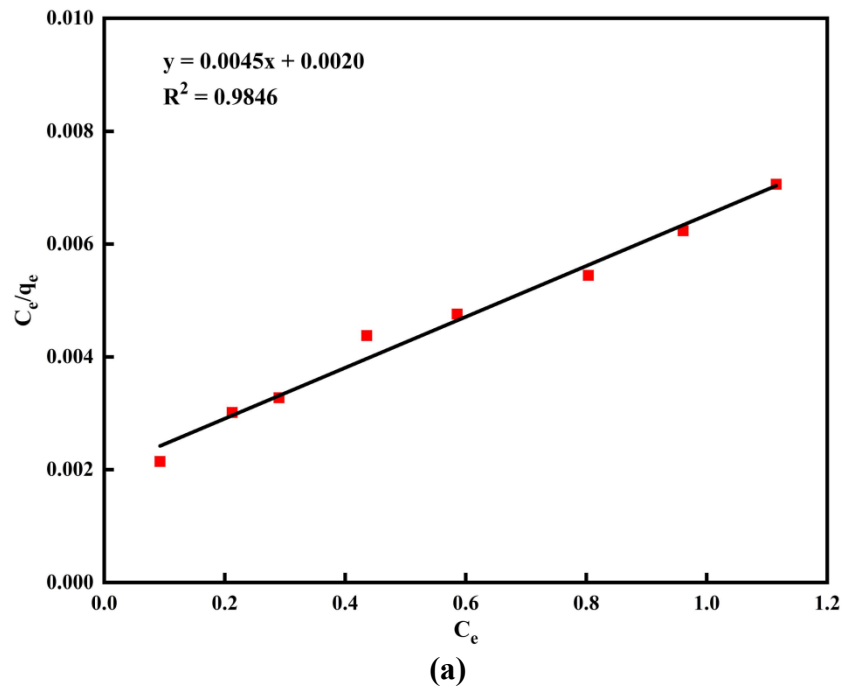


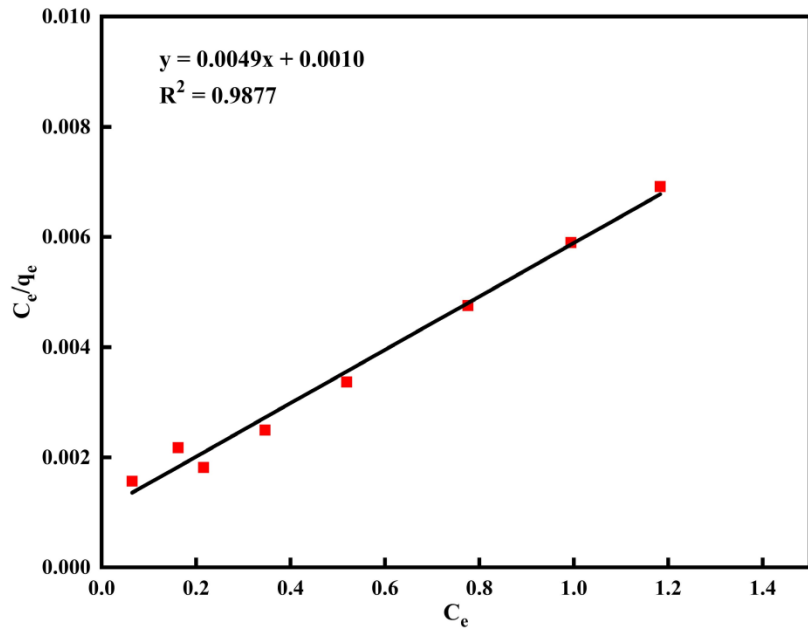
(b)



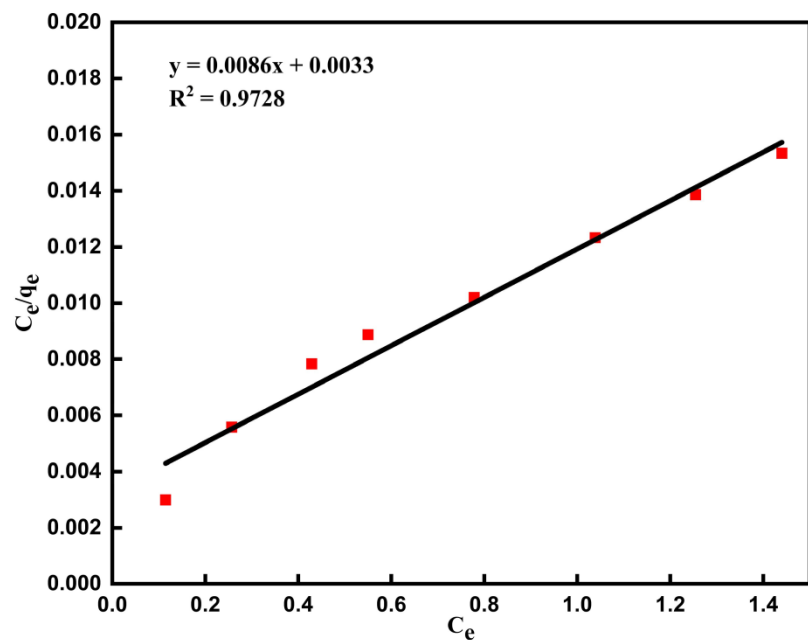
(c)

Fig. S18 Effect of palladium(II) concentration and temperature on the adsorption by (a) UiO-66-NH₂ (b) Zr-Zn-MOF-2 (c) Zr-Zn-MOF-3

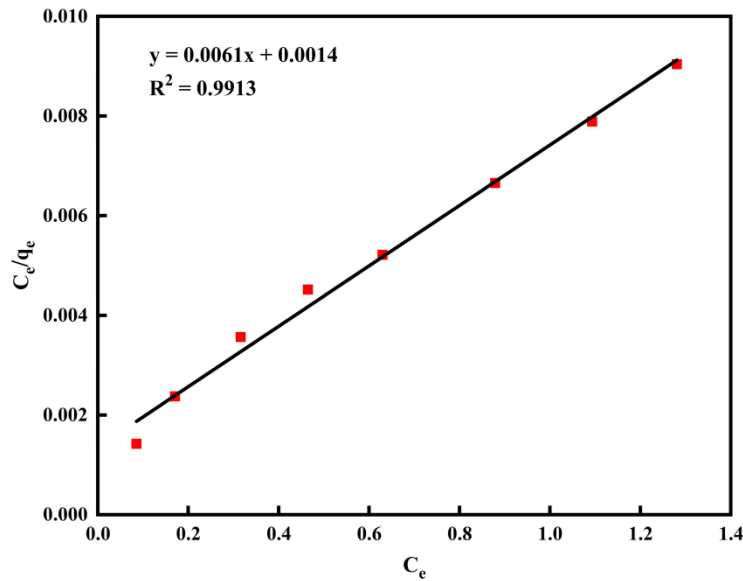




(b)



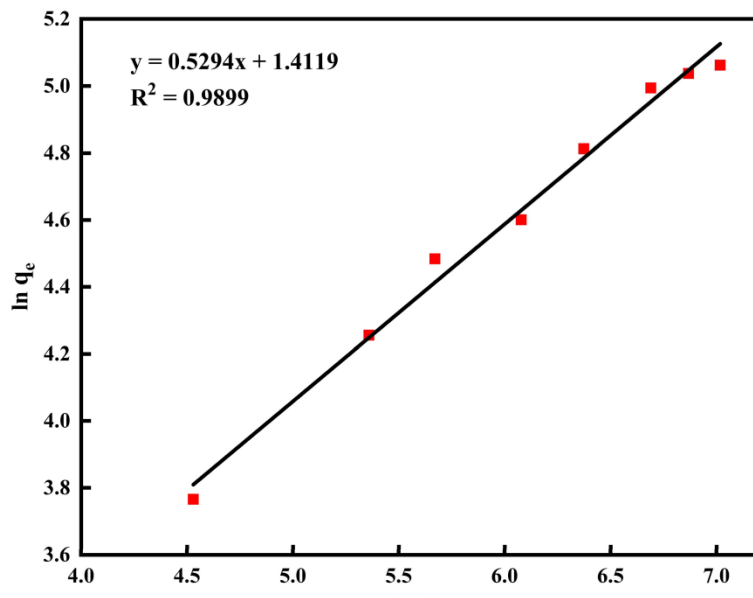
(c)



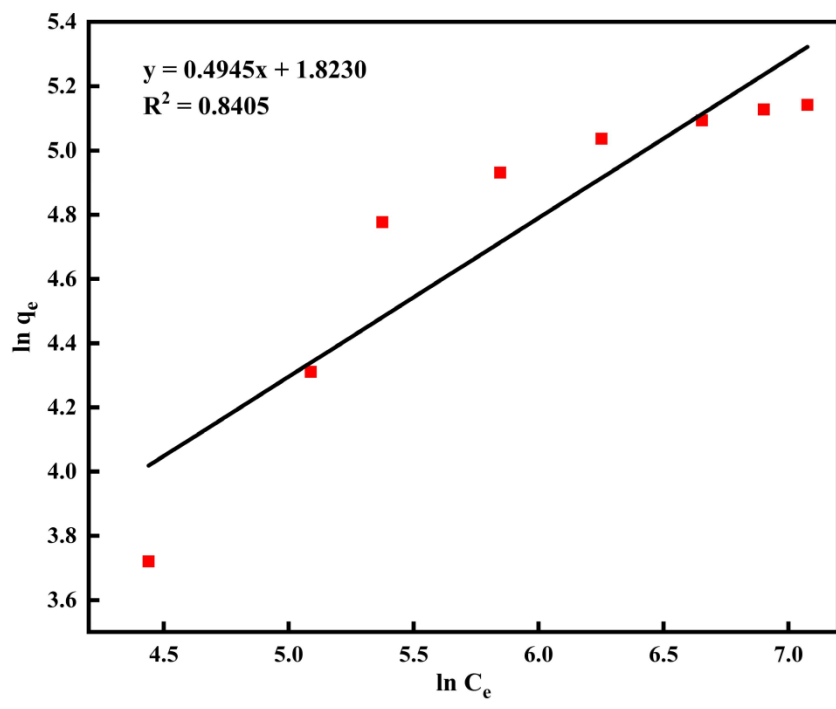
(d)

Fig S19. Linear Langmuir isotherm for the adsorption of palladium(II) on different MOFs

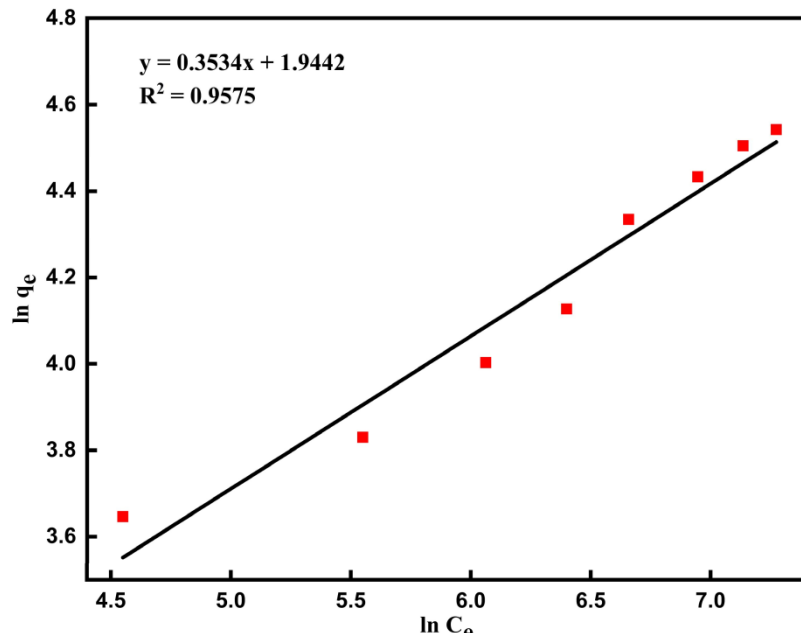
(a) UiO-66-NH₂ (b) Zr-Zn-MOF-1 (c) Zr-Zn-MOF-2 (d) Zr-Zn-MOF-3



(a)



(b)



(c)

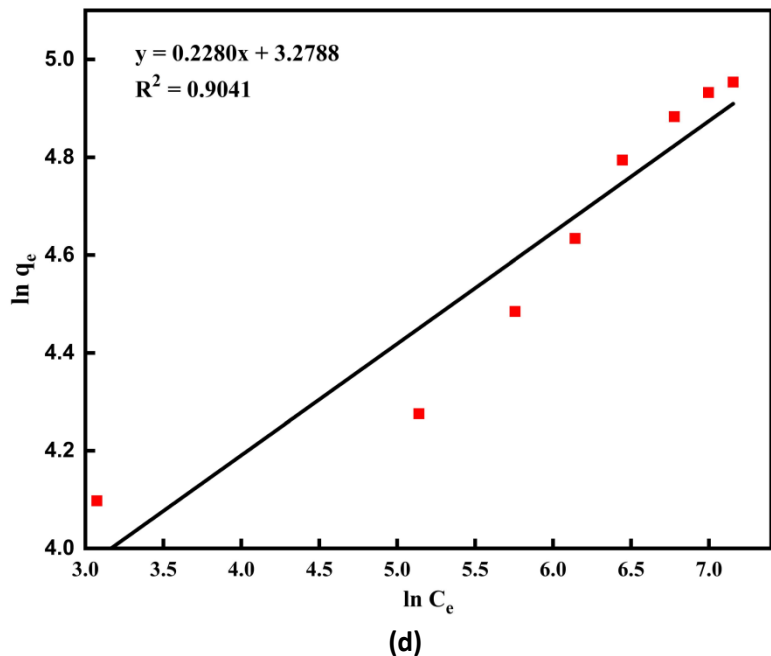
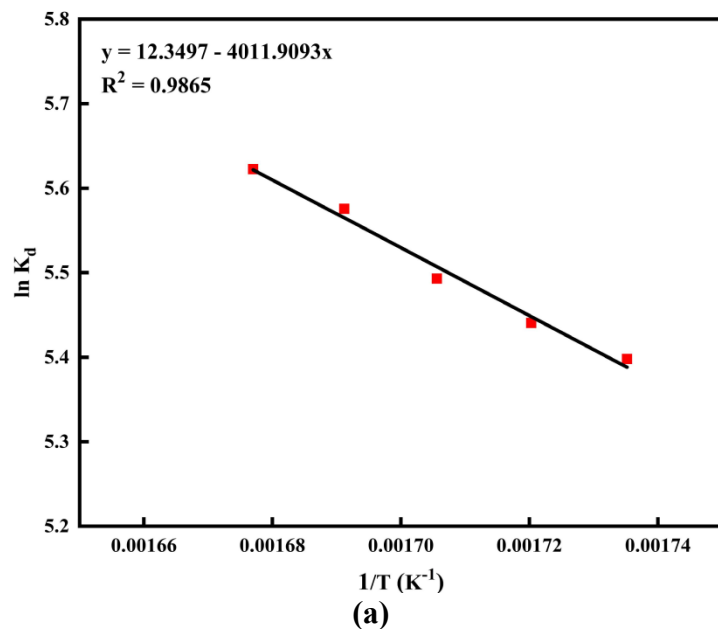
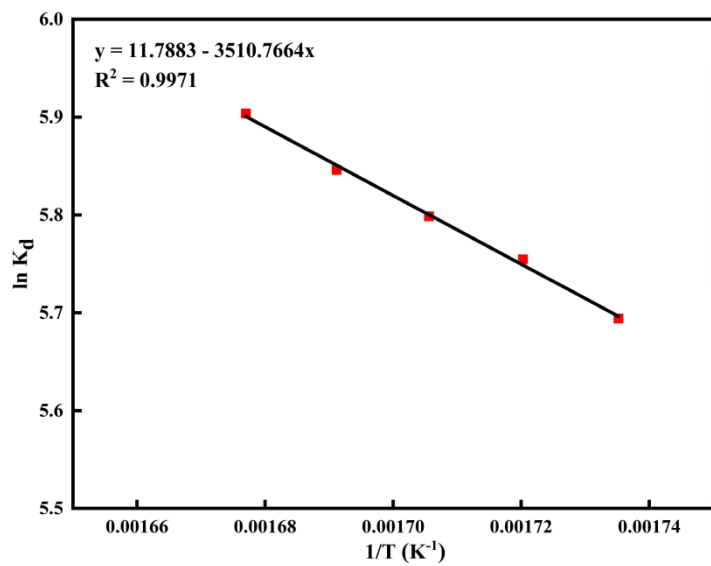


Fig S20. Linear Freundlich isotherm for the adsorption of palladium(II) on different MOFs

(a) UiO-66-NH₂ (b) Zr-Zn-MOF-1 (c) Zr-Zn-MOF-2 (d) Zr-Zn-MOF-3





(b)

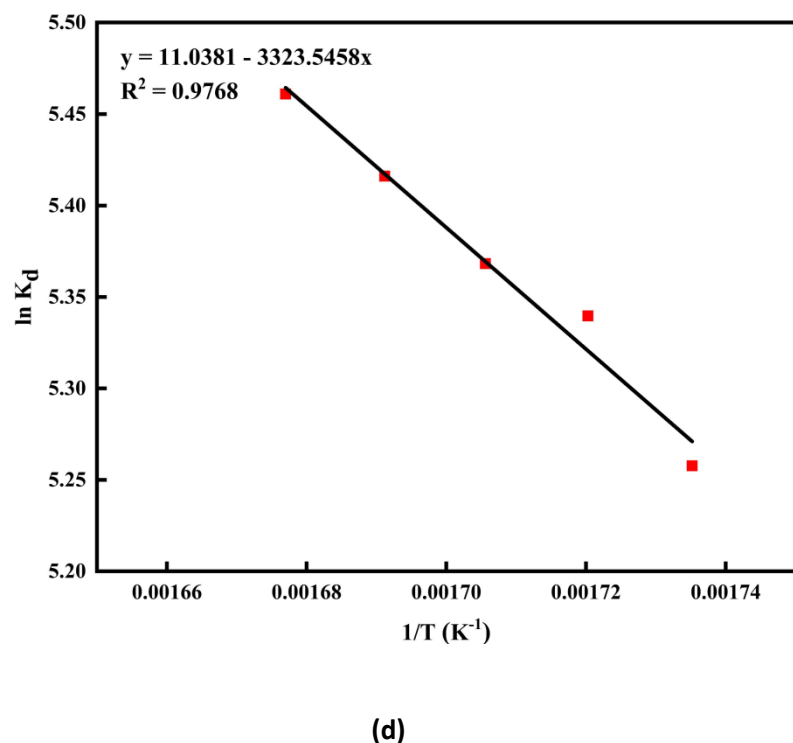
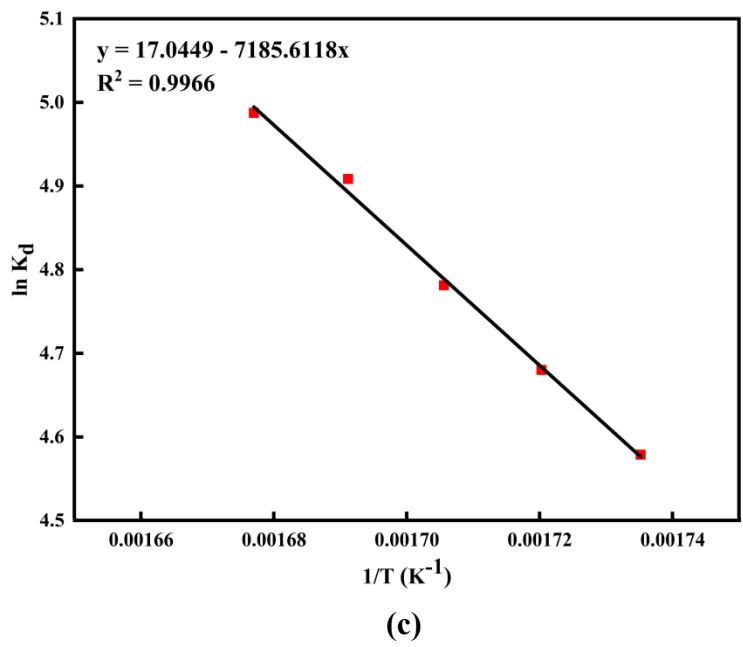


Fig. S21 $\ln K_d$ versus $1/T$ (a) UiO-66-NH₂ (b) Zr-Zn-MOF-1 (c) Zr-Zn-MOF-2 (d) Zr-Zn-MOF-3

References:

1. S. P. Sangal and A. K. Dey, Microdetermination of palladium (II) using 1-(o-
arsonophenylazo)-2-naphthol-3, 6-disulfonate (thoron) as a colorimetric reagent,
Microchemical Journal, 1963, **7**, 257-262.